



HAL
open science

The Role of Volume Fraction and Additives on the Rheology of Suspensions of Micron Sized Iron Particles

Georges Bossis, Olga Volkova, Yan Grasselli, Alain Cifreio

► **To cite this version:**

Georges Bossis, Olga Volkova, Yan Grasselli, Alain Cifreio. The Role of Volume Fraction and Additives on the Rheology of Suspensions of Micron Sized Iron Particles. *Frontiers in Materials*, 2019, 6, 10.3389/fmats.2019.00004 . hal-03447638

HAL Id: hal-03447638

<https://hal.science/hal-03447638>

Submitted on 24 Nov 2021

HAL is a multi-disciplinary open access archive for the deposit and dissemination of scientific research documents, whether they are published or not. The documents may come from teaching and research institutions in France or abroad, or from public or private research centers.

L'archive ouverte pluridisciplinaire **HAL**, est destinée au dépôt et à la diffusion de documents scientifiques de niveau recherche, publiés ou non, émanant des établissements d'enseignement et de recherche français ou étrangers, des laboratoires publics ou privés.



The Role of Volume Fraction and Additives on the Rheology of Suspensions of Micron Sized Iron Particles

Georges Bossis^{1*}, Olga Volkova¹, Yan Grasselli^{1,2} and Alain Cifreo¹

¹ Laboratory Inphyni, Institute of Physics of Nice, CNRS, University of Nice Sophia-Antipolis, Nice, France, ² SKEMA Business School, Université Côte d'Azur, Sophia Antipolis, France

OPEN ACCESS

Edited by:

Seung-Bok Choi,
Inha University, South Korea

Reviewed by:

Xufeng Dong,
Dalian University of Technology (DUT),
China

Evguenia Korobko,

A.V. Luikov Heat and Mass Transfer
Institute (NASB), Belarus

*Correspondence:

Georges Bossis
bossis@unice.fr

Specialty section:

This article was submitted to
Smart Materials,
a section of the journal
Frontiers in Materials

Received: 29 October 2018

Accepted: 10 January 2019

Published: 08 February 2019

Citation:

Bossis G, Volkova O, Grasselli Y and
Cifreo A (2019) The Role of Volume
Fraction and Additives on the
Rheology of Suspensions of Micron
Sized Iron Particles. *Front. Mater.* 6:4.
doi: 10.3389/fmats.2019.00004

The increase of the yield stress vs. the magnetic field is the most important quantity characterizing the efficiency of a magnetorheological suspension. The theory based on the formation of columnar aggregates predicts a linear variation with the volume fraction of magnetic particles. In this paper we review previous models used to calculate forces and yield stress and will introduce a new model based on rupture at zero strain. Predictions of these models are compared with the experimental data obtained for carbonyl iron particles, by different authors. Whereas, previous analytical prediction strongly overestimates experimental yield stress, those calculated using the Finite Element Method (FEM), together with affine trajectories, reproduce the experiments well and show a linear dependence with the volume fraction and a $H^{3/2}$ behavior between 50 and 200 kA/m. Nevertheless, at very high-volume fractions (>55%), where the suspension can only flow in the presence of specific additives, the dependence of the yield stress vs. the volume fraction and the magnetic field is dramatically changed. We observed a jamming transition, which is triggered by the application of a low magnetic field and which depends strongly on the volume of the fraction. Here, we will discuss new perspectives arising from the use of these very high-volume fractions.

Keywords: carbonyl iron, yield stress, discontinuous shear thickening, jamming, magnetorheology

INTRODUCTION

Magnetorheological (MR) suspensions are smart fluids made of magnetizable particles, with a typical size varying between 100 nm and a few microns dispersed in a carrier liquid, which can be mineral oil, silicone oil, ethylene glycol, etc. The interest of these fluids is their rapid and reversible transformation in a solid when they are submitted to a magnetic field. This transformation occurs due to the attractive interaction of a dipolar nature, generated by the magnetization of the particles. The solid phase is characterized by its resistance to a shear strain, namely the yield stress, over which the solid begins to creep. Most applications look for fluids that present the highest possible yield. Of course, the higher the magnetic field, the higher the yield stress, with the limit of the full magnetization of the particles as well as the inconvenience of weight and place that are necessary for the coils to produce a high magnetic field. Besides the importance of a high yield stress, other requisites are also important for industrial uses such as easy resuspension after sedimentation and a low off state viscosity. In order to obtain a high yield stress and a reversible magnetization,

very few materials are available, and in practice industrial MR fluids are based on carbonyl iron particles as they present a high saturation magnetization and are synthesized in large quantities to produce sintered magnetic circuits. Iron particles have the inconvenience of high density and therefore of rapid sedimentation; furthermore, due to the pressure generated by their weight and the attractive Van der Waals forces, they easily aggregate irreversibly. In order to prevent this irreversible aggregation, coating of the particles by some molecules (surfactant, polymer, even ions) is necessary. Many papers and patents describe these formulations and their effects in reducing sedimentation and aggregation [for a recent review see reference (Ashtiani et al., 2015)]. This coating, which prevents the particles to come into close contact can also present the inconvenience of lowering the magnetic force, which strongly depends on the distance between the particles. Ultimately however, despite decades of research, the maximum yield stress of commercial fluids remains in the 40–60 kPa range for a 0.3–0.5 Tesla magnetic field induction. We first take a look at the yield stresses predicted by the available models and compare these predictions with the experimental data, then, in light of recent experimental results involving frictional stresses, we will focus on the performance of these fluids and how they can be improved.

PREDICTION OF THE YIELD STRESS

The cohesion of the solid phase, and therefore its yield stress, depends first on the strength of the magnetic forces developed between the particles, and second on the structure and its evolution under combined magnetic and hydrodynamic forces. We briefly review the main models and then compare their prediction, both for the forces between the particles and for the yield stress. To do this analysis we take a look at the magnetic properties of the carbonyl iron particles, those currently used in practical applications. The magnetization curve is described by the Frolich Kennelly equation: $M = M_s \chi_i H / (M_s + \chi_i H)$ Where M_s is the saturation magnetization and χ_i the initial permeability. For the saturation magnetization we have taken the pure iron: $M_s = 1,680$ kA/m and the initial permeability $\chi_i = 70$ (De Vicente et al., 2002).

Magnetic Forces Between Two Particles

Contrary to well-known dipolar approximation, a multipolar approach for two particles, first presented by Klingenberg (Klingenberg and Zukoski, 1990) and then for several particles described in subsequent works (Clercx and Bossis, 1993), gives an exact prediction of the force for a linear magnetization. The result for two particles reads:

$$F_m(\vec{r}) = 12\pi\mu_0 a^2 \beta^2 H^2 \left(\frac{a}{r}\right)^4 \left[(2f_{//} \cos^2(\theta) - f_{\perp} \sin^2(\theta)) \vec{e}_r + f_r \sin(2\theta) \vec{e}_\theta \right] \quad \text{with } \beta = \frac{\mu_p - 1}{\mu_p + 2} \quad (1)$$

In Equation (1) a is the radius of the particles, μ_p their relative permeability given by $\mu_p = 1 + M/H$ and $f_{//}$, f_{\perp} , f_r are functions of the initial permeability: $\mu_i = \chi_i + 1$ and of the

normalized separation between the surfaces of the two particles $\varepsilon = r/a - 2$ (cf **Figure S1**). A **Table S2** of these functions for different separations and different values of χ_i is provided in the **Supplementary Material**.

A popular model derived in Ginder et al. (1996) uses, on the contrary, the approximation that the pole of the particles is completely saturated (cf **Figure S1**) in a zone defined by $\rho = \delta$ where ρ is the polar coordinate. The interparticle force coming from the integral of the magnetic stress tensor is then given by:

$$F_r = \frac{\mu_0}{2} \int_0^W (H(\rho) - H)^2 2\pi\rho d\rho \quad \text{with } H(\rho) = H \frac{(2 + \varepsilon)}{\varepsilon + \rho^2} \quad \text{for } \rho > \delta \text{ and } H(\rho) = M_s \text{ for } \rho < \delta \quad (2)$$

The value of δ is obtained from the equality between the two expressions for $\rho = \delta$ which gives: $\delta = \sqrt{2H/M_s - \varepsilon}$

In these expressions the distances are normalized by the radius of the sphere and W is of order unity. In the limit where $\varepsilon/2 < H/M_s \ll 1$, the upper bound of the integral is negligible and we obtain:

$$F_{ra} = \pi\mu_0 a^2 M_s^2 \left(\frac{2H}{M_s} - \frac{\varepsilon}{2} \right) \quad (3)$$

It is possible to check the validity of this approximation, using a finite element method (FEM) for the calculation of the magnetic field. We have used the FEMM software to calculate the force between two spheres placed in a constant magnetic field H :

$$F_{rFEM} = 2\pi a^2 \int_0^\pi [\sigma_{rr} \cos(\theta) - \sigma_{r\theta} \sin(\theta)] \sin(\theta) d\theta \quad (4)$$

with $\sigma_{rr} = \mu_0(\mu_f H_r^2 - 0.5H^2)$ $\sigma_{r\theta} = \mu_0\mu_f H_r H_\theta$

In our case the carrier liquid was non-magnetic and so $\mu_f = 1$. The fields H_r and H_θ are the field normal and tangential to the internal surface of the particle, respectively. In **Figure S2**, we have compared the dependence of these three models on the amplitude of the magnetic field for a separation distance of 0.01a and a radius of 1 mm. As shown in this figure, the multipolar force (Equation 1) and the FEM calculation (Equation 4) gave the same result at low field as expected but above $H = 25$ kA/m, the multipolar model overestimates the force. The analytical model (Equation 3) largely overestimates the force. This force calculation is necessary to predict the yield stress, but we also need to know the structure and its deformation under strain.

Models for the Yield Stress

Affine Trajectories

In the standard model the particles are supposed to follow trajectories which are affine with the imposed shear flow. The magnetic field is perpendicular to the imposed flow (cf **Figure S1**). The equilibrium position of the particles is obtained by balancing the shear stress on the top particle with the magnetic restoring force. When the two representative particles are aligned with the magnetic field ($\theta = 0$ on **Figure S1**) the gap between the

surfaces is given by the thickness of the coating layer, typically of the order of a few nanometers. When particle 2 moves along the stream line, the gap increases with the strain: $\gamma = \tan(\theta)$ as: $\varepsilon - \varepsilon_0 = 2(\sqrt{1 + \gamma^2} - 1)$. On the other hand, the magnetic force along the x axis is $F_r \sin\theta \cos^2\theta$ where F_r is the radial force calculated in the preceding section for particles aligned in the direction of the field. In a model where all particles form chains spanning the gap with a surface density $n_c/S = 2a N/V = (3/2)\Phi/(\pi a^2)$, with Φ the volume fraction, the shear stress is given by:

$$\tau(\gamma) = \frac{3}{2} \Phi \max\left(\frac{F_r}{\pi a^2} \sin\theta \cos^2\theta\right) = \frac{3}{2} \Phi \max\left(\frac{F_r(\gamma)}{\pi a^2} \frac{\gamma}{(1 + \gamma^2)^{3/2}}\right) \quad (5)$$

For the analytical expression of the force Equation (3), we get, (always for $\varepsilon/2 < H/M_s < < 1$):

$$\tau_{ya} = \sqrt{16/3} \Phi \mu_0 M_s H^{3/2} \quad (6)$$

Equation (6) differs slightly from that given in Ginder et al. (1996) where the prefactor is $\sqrt{6}$. It is worth noting that when the magnetization of the particles is saturated, the force between the particles is obtained from interactions between rigid dipoles $m = M_s v$, where v is the volume of the particle. The results for the yield stress is readily derived, for non-interacting particle chains (Ginder et al., 1996) as: $\tau_{y\max} = 0.086 \Phi \mu_0 M_s^2$.

For the multipolar force we need to interpolate the tables $f_{//}$, f_{\perp} , f_r as a function of the separation and, in the non-linear case derived by FEM, it is also needed to do this interpolation for each value of the field; the data used are given in Table S3. The results are presented in Figure 1A but, before discussing them, it is worth introducing another model, which to our knowledge, has never been used for MR (or ER) fluids.

Rupture at Zero Strain

Here we suppose that the particles are packed in some disordered way, and that the solid phase will yield suddenly when the shear stress is high enough to separate the particles on a given “cutting” plane which, in a simple shear, is perpendicular to the velocity gradient. This kind of model is used to predict the yield stress of suspensions of particles aggregated in the presence of Van der Waals forces (Scales et al., 1998). The only difference in our case is that the interparticle force is proportional to $(H \cos\theta)^2$ instead of being independent of θ . Otherwise the interparticle distances are supposed to be distributed isotropically, which is mainly true at a high-volume fraction. Following the same steps as in Scales et al. (1998) we obtain:

$$\tau_y = \frac{3\Phi K(\Phi)}{20\pi R^2} F_r(\varepsilon_0) \quad \text{with} \quad K(\Phi) = 36\Phi/\pi \quad (7)$$

The factor $3/20$ comes from the $\cos^2\theta$ instead of $1/4$ for an isotropic force. The function $K(\Phi)$ is the coordination number taken from Suzuki et al. (1981) and ε_0 is the minimum gap between two particles.

Comparison of the Different Models

The predictions of the different models are reported in Figure 1A. Firstly if we compare, in the affine model, the predictions related to the 3 different approximations of forces: Equations (1, 3, 4), we recover the fact that the multipolar model gives a rather good prediction for low fields but, due to the linear magnetization hypothesis, highly overestimates the yield stress at high fields. The analytic expression overestimates the yield stress given by FEM, by about one order of a magnitude. Lastly, the model of rupture at zero strain (Equation 7), is calculated with the force F_r obtained by FEM for $\varepsilon = 0.002$, which is a reasonable value considering a coating layer of 2 nm and a radius of $1 \mu\text{m}$. The corresponding prediction is well-above the FEM prediction and is, by chance, quite close to that of the analytical model. It should also be noted that the fit of the yield stress by a power law: $\tau_y = K \cdot H^n$ provides a good fit with $n = 1.94$ ($R^2 = 0.9997$) only for $H \leq 50 \text{ kA/m}$ (Figure S3) which is three times smaller than the field used for the transition from H^2 to $H^{3/2}$ ($H_c = 151 \text{ kA/m}$ in Fang et al. (2009)). It is also worth noting that the radial force, at contact between two particles, increases steadily in the range of $\varepsilon = 0-0.01$ (cf Table S2), which may explain, at least in the rupture model, the decrease of the yield stress in the presence of a coating layer (Cvek et al., 2018). This comparison of the models was done for two spheres in a given field, which

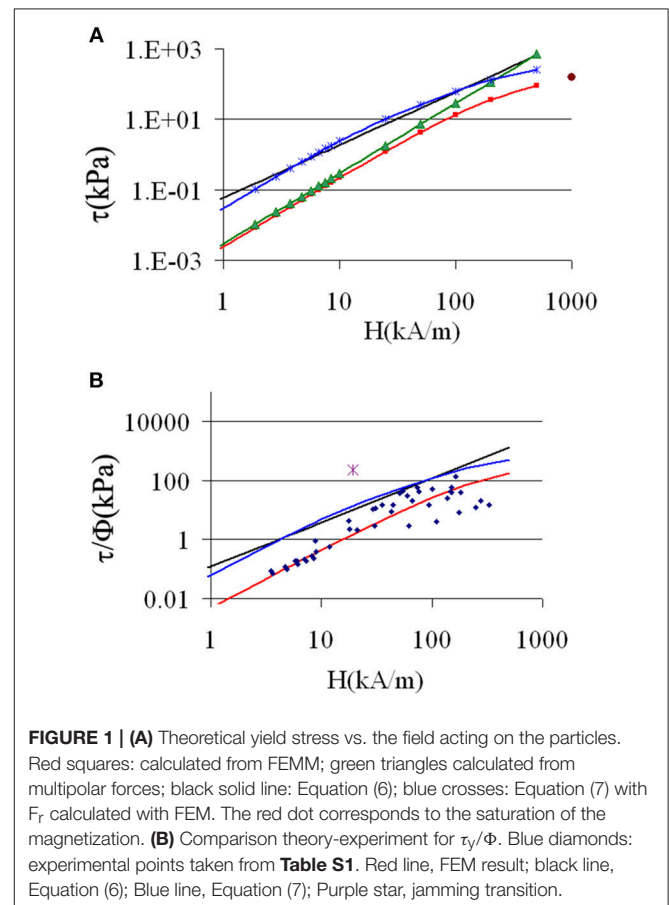


FIGURE 1 | (A) Theoretical yield stress vs. the field acting on the particles. Red squares: calculated from FEMM; green triangles calculated from multipolar forces; black solid line: Equation (6); blue crosses: Equation (7) with F_r calculated with FEM. The red dot corresponds to the saturation of the magnetization. **(B)** Comparison theory-experiment for τ_y/Φ . Blue diamonds: experimental points taken from Table S1. Red line, FEM result; black line, Equation (6); Blue line, Equation (7); Purple star, jamming transition.

we consider as the average field, in order to compare with the experiments in the next section. Some numerical results for the yield stress of a set of particles can be obtained with a good precision in a multipolar approach, even for high permeability, but for particles distributed on a periodic network (Clercx and Bossis, 1993) with an affine deformation. In this case all the particles are separated by the same gap, which is an unphysical and unstable structure. It is also possible to use a double chain structure so that it can deform and still keep contacts and stability, but it underestimates the yield stress (López-López et al., 2012) and also can't be used in numerical simulations. In fact, almost all numerical simulations of MR suspensions use the dipolar approximation, which largely underestimates the magnetic force (Clercx and Bossis, 1993). We have found one paper (Lacis and Gosko, 2009) using an expression similar to Equation (1), with some tables derived from FEM simulations for two particles and another based on FEM simulations between several particles in a single chain (Kang et al., 2012). A simulation method, called smooth particle dynamics (Hashemi et al., 2016, 2018), can also be used to solve the magnetostatics equation between several particles, but is restricted to a few particles with a rather small (<10) susceptibility. As discussed in the next section, the use of a magnetic force derived from FEM, calculated with a very fine mesh for two particles, is quite realistic and certainly much more efficient in terms of computing time.

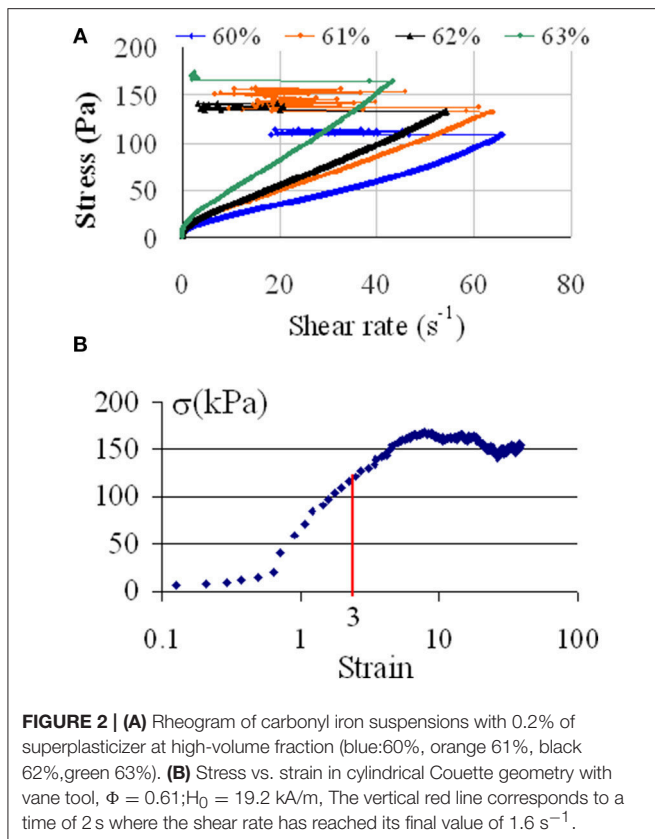
COMPARISON WITH EXPERIMENTS

Comparing these predictions with experimental data is not so simple as, very often, the knowledge of the experimental conditions is incomplete. We have selected data concerning carbonyl iron particles (CI) whose magnetization curve of the powder is rather well-established with a saturation magnetization of 200 emu/g. Usually the experiments are made in plate-plate geometry, with the field perpendicular to the plate. In order to compare with the theory, we must first consider that the field inside the suspension is $H=H_0/\mu(H)$, where H_0 is the external field measured in the absence of suspension and $\mu(H)$ the permeability of the suspension. We have deduced the magnetization curve of CI particles from a measurement of $M(H)$ at a volume fraction: $\Phi = 64\%$. This magnetization curve of CI particles is well-fitted in the range 0–400 kA/m by a Langevin curve: $M_1(H)=(\coth(cH)-1/cH)M_{sr}$ with $c = 0.014$ and $M_{sr} = 1750$ kA/m. This last value is slightly higher than the saturation magnetization of CI ($M_s \approx 1600$ kA/m) due to a shift of the fit for $H>400$ kA/m. The magnetization at any volume fraction of the suspension is obtained by replacing M_{sr} by $M_{sr}\cdot\Phi$ and we have checked that it works well-even at low Φ , for instance for $\Phi = 0.2$ and $\Phi = 0.32$ BASF. The permeability for any given volume fraction is then: $\mu(H) = 1+M_1(H)\cdot\Phi/H$. The second point we need to take into account is that, in the plate-plate configuration, the yield stress provided by the software is overestimated by a factor of 4/3 (Bossis et al., 2002; Laun et al., 2010). The data collected in different publications (Kordonski and Golini, 1999; Chin et al., 2001; Lim et al., 2004; Jang et al., 2005; Cheng et al., 2009; Ierardi and Bombard, 2009; Laun et al., 2010; Kim et al.,

2012; Bombard et al., 2015; Esmaeilnezhad et al., 2017; Dong et al., 2018; Plachy et al., 2018) are reported in **Table S1** and plotted in **Figure 1B** (blue diamonds). There is a considerable scatter of the data, but it appears clearly that the affine model with the calculation of forces through FEM (red curve), provides the best prediction compared to both Equation (6) and Equation (7). Now, we draw the attention on the single point (purple cross) above all the curves in **Figure 1B** which is the result of a jamming transition.

JAMMING TRANSITION AT HIGH VOLUME FRACTION

Jamming transition, also known as discontinuous shear thickening (DST), was observed in highly concentrated suspensions of solid non-Brownian particles like ceramics (Bergström, 1998), cornstarch (Fall et al., 2008, 2015) and also in model suspensions made of PMMA (Pan et al., 2015) or silica particles (Lootens et al., 2003) and calcium carbonate (Bossis et al., 2017). In the two last systems, superplasticizer molecules, common in the cement industry, were used as surfactants. We have recently found that by using, for instance, a polyoxyethylene polyphosphonate (Bossis et al., 2017), we can reach volume fractions of CI particles in water larger than 60%, still keeping a low yield stress and a viscosity of 1-2Pa.s. Now the rheogram at the zero field presents a singularity at a critical stress, where the shear rate abruptly decreases during a ramp of stress (**Figure 2A**). This DST phenomenon is due to the transition of a lubricated regime to a frictional one (Mari et al., 2014; Wyart and Cates, 2014). Above this point the shear rate fluctuates around some low values. We also see on this graph that, by increasing the volume fraction, the critical stress increases and the critical shear rate decreases. These critical values are obtained at zero magnetic field, but when the field is increased for a given volume fraction, the critical shear rate will continuously decrease to zero in a field range typically of 0–20 kA/m (Bossis et al., 2016). If instead of applying a ramp of stress we apply a ramp of shear rate, at the critical point we then obtain a jump of stress to very high values which overcomes the range of conventional rheometers. This is the purple point in **Figure 1B**, which was obtained in the presence of a field of 19.2 kA/m. The corresponding evolution of stress is plotted in **Figure 2B** vs. the strain. It was obtained in a cylindrical Couette flow with a vane tool and a homemade rheometer to be able to measure high torques (Bossis et al., 2016). The shear rate was increased from 0 to 1.6 s^{-1} in 2 s then kept constant for 25 s. The stress does not grow until the strain reaches a value around one and then increases up to 150 kPa where it remains constant afterwards. The interesting point is that this transition from a normal regime to this frictional regime can be controlled by the application of a low magnetic field (a few kA/m), thus opening the door for new applications of MR fluids. It is worth noting that a very high value of yield stress in a MR fluid was previously attained in another way, which also mobilizes the friction between particles, but with the help of a lateral pressure obtained by the compression of the suspension of the initial volume fraction $\Phi = 45\%$ by sliding wedges (Tao,



2001). As reported in numerous previous works, [for instance (Ashtiani et al., 2015; Cvek et al., 2018)] the additives are used to stabilize the particles against corrosion and sedimentation; they can either increase the yield stress through a better compaction of the local structure [term $K[\Phi]$ in Equation (7)], or decrease it if the coating layer is too thick [term $F_r(\epsilon_0)$ in Equation (7)]. In our case it plays a key role due its expulsion from the surface, which provokes the jamming transition

CONCLUSION

In this paper we have briefly reviewed the models of yield stress under the hypothesis of affine displacement of the particles and have also proposed a new approach based on a rupture model. It appears that the affine motion, with a calculation of the forces through FEM simulation, provides the best agreement with the experimental data of τ_y/Φ , collected for carbonyl iron suspensions. The commonly used Equation (6) strongly overestimates the experimental results but its prediction of a

REFERENCES

Ashtiani, M., Hashemabadi, S. H., and Ghaffari, A. (2015). A review on the magnetorheological fluid preparation and stabilization. *J. Magn. Magn. Mater.* 374, 716–730. doi: 10.1016/j.jmmm.2014.09.020

regime $\tau_y \propto H^{3/2}$ is verified between ~ 50 and 200 kPa. No model is able to predict the high value of stress at low field obtained in suspensions of very high-volume fractions: $\Phi > 0.6$. In this case, it is the abrupt transition toward a frictional regime after expulsion of a superplasticizer layer, which leads to very high values of stress. This transition is obtained either above a critical magnetic field or above a critical shear rate, which opens up new perspectives for applications that require a strong response with a small field.

AUTHOR CONTRIBUTIONS

GB, OV, YG, and AC contributed conception and design of the study. GB wrote the first draft of the paper. OV found and organized the references and the figures. YG filled the database of the previous works on the subject and AC contributed to the theoretical part. All authors contributed to manuscript revision, read and approved the submitted version.

FUNDING

Center National d'Etudes Spatiales (CNES, the French Space Agency).

ACKNOWLEDGMENTS

This work was supported by the Center National d'Etudes Spatiales CNES. We also thank the mechanical workshop of our institute for fabricating part of our home made rheometer.

SUPPLEMENTARY MATERIAL

The Supplementary Material for this article can be found online at: <https://www.frontiersin.org/articles/10.3389/fmats.2019.00004/full#supplementary-material>

Figure S1 | Schematic of the notations for two particles in a magnetic field.

Figure S2 | Force vs. magnetic field for a separation $\epsilon = 0.01$; black line: analytic expression: Equation (3); green triangles: multipolar approach: Equation (1); red triangles: FEM, Equation (4).

Figure S3 | Power law fit of the FEM result for the normalized yield stress τ_y/Φ . Red solid line: power law with $n = 1.94$; blue solid line: power law with $n = 3/2$; red crosses: FEM result; black solid line: Equation (6).

Table S1 | Corrected experimental yield stress normalized by the volume fraction (column E) in kPa vs. the Maxwell field in the suspension (column H) in kA/m.

Table S2 | Coefficients of the force in Equation (1) for different values of $\alpha = \mu_p/\mu_f$ vs. the gap ϵ .

Table S3 | Values of the force obtained with the free software FEMM for different fields and separations between two spheres. The parameters for the fit vs. the normalized separation, ξ , (< 0.2) are given for each field.

BASF (2010). *Technical Data Sheet MR2899*.

Bergström, L. (1998). Shear thinning and shear thickening of concentrated ceramic suspensions. *Colloids Surf. A* 133, 151–155. doi: 10.1016/S0927-7757(97)00133-7

Bombard, A. J., Gonçalves, F. R., and de Vicente, J. (2015). Magnetorheology of carbonyl iron dispersions in 1-Alkyl-3-methylimidazolium ionic

- liquids. *Ind. Eng. Chem. Res.* 54, 9956–9963. doi: 10.1021/acs.iecr.5b02824
- Bossis, G., Boustingorry, P., Grasselli, Y., Meunier, A., Morini, R., Zubarev, A., et al. (2017). Discontinuous shear thickening in the presence of polymers adsorbed on the surface of calcium carbonate particles. *Rheol. Acta* 56, 415–430. doi: 10.1007/s00397-017-1005-4
- Bossis, G., Grasselli, Y., Meunier, A., and Volkova, O. (2016). Outstanding magnetorheological effect based on discontinuous shear thickening in the presence of a superplasticizer molecule. *Appl. Phys. Lett.* 109:111902. doi: 10.1063/1.4962467
- Bossis, G., Volkova, O., Laciš, S., and Meunier, A. (2002). “Magnetorheology: fluids, structures and rheology,” in *Ferrofluids, Part of Lecture Notes in Physics, Vol. 594* (Springer), 202–230.
- Cheng, H. B., Wang, J. M., Zhang, Q. J., and Weryley, N. M. (2009). Preparation of composite magnetic particles and aqueous magnetorheological fluids. *Smart Mater Struct.* 18:085009. doi: 10.1088/0964-1726/18/8/085009
- Chin, B. D., Park, J. H., Kwon, M. H., and Park, O. O. (2001). Rheological properties and dispersion stability of magnetorheological (MR) suspensions. *Rheologica Acta* 40, 211–219. doi: 10.1007/s003970000150
- Clercx, H. J. H., and Bossis, G. (1993). Electrostatic interactions in slabs of polarizable particles. *J. Chem. Phys.* 98, 8284–8293. doi: 10.1063/1.464534
- Cvek, M., Mrlik, M., Moucka, R., and Sedlacik, M. (2018). A systematic study of the overall influence of carbon allotrope additives on performance, stability and redispersibility of magnetorheological fluids. *Colloids Surf. A* 543, 83–92. doi: 10.1016/j.colsurfa.2018.01.046
- De Vicente, J., Bossis, G., Laciš, S., and Guyot, M. (2002). Permeability measurements in cobalt ferrite and carbonyl iron powders and suspensions. *J. Magn. Mater.* 251, 100–108. doi: 10.1016/S0304-8853(02)00484-5
- Dong, Y. Z., Piao, S. H., Zhang, K., and Choi, H. J. (2018). Effect of CoFe₂O₄ nanoparticles on a carbonyl iron based magnetorheological suspension. *Colloids Surf. A* 537, 102–108. doi: 10.1016/j.colsurfa.2017.10.017
- Esmailnezhad, E., Jin Choi, H., Schaffie, M., Gholizadeh, M., Ranjbar, M., and Hyuk Kwon, S. (2017). Rheological analysis of magnetite added carbonyl iron based magnetorheological fluid. *J. Magnetism Magnetic Mater.* 444, 161–167. doi: 10.1016/j.jmmm.2017.08.023
- Fall, A., Bertrand, F., Hautemayou, D., Mézière, C., Moucheront, P., Lemaitre, A., et al. (2015). Macroscopic discontinuous shear thickening versus local shear jamming in cornstarch. *Phys. Rev. Lett.* 114:098301. doi: 10.1103/PhysRevLett.114.098301
- Fall, A., Huang, N., Bertrand, F., Ovarlez, G., and Bonn, D. (2008). Shear thickening of cornstarch suspensions as a reentrant jamming transition. *Phys. Rev. Lett.* 100:018301. doi: 10.1103/PhysRevLett.100.018301
- Fang, F. F., Choi, H. J., and Jhon, M. S. (2009). Magnetorheology of soft magnetic carbonyl iron suspension with single-walled carbon nanotube additive and its yield stress scaling function. *Colloids Surf. A* 351, 46–51. doi: 10.1016/j.colsurfa.2009.09.032
- Ginder, J. M., Davis, L. C., and Elie, L. D. (1996). Rheology of magnetorheological fluids: models and measurements. *Int. J. Mod. Phys. B* 10, 3293–3303. doi: 10.1142/S0217979296001744
- Hashemi, M. R., Manzari, M. T., and Fatehi, R. (2016). A SPH solver for simulating paramagnetic solid fluid interaction in the presence of an external magnetic field. *Appl. Math. Model.* 40, 4341–4369. doi: 10.1016/j.apm.2015.11.020
- Hashemi, M. R., Manzari, M. T., and Fatehi, R. (2018). Direct numerical simulation of magnetic particles suspended in a Newtonian fluid exhibiting finite inertia under SAOS. *J. Non-Newtonian Fluid Mech.* 256, 8–22. doi: 10.1016/j.jnnfm.2018.03.004
- Ierardi, R. F., and Bombard, A. J. (2009). Off-state viscosity and yield stress optimization of magneto-rheological fluids: a mixture design of experiments approach. *J. Phys. Conf. Series* 149:012037. doi: 10.1088/1742-6596/149/1/012037
- Jang, I. B., Kim, H. B., Lee, J. Y., You, J. L., Choi, H. J., and Jhon, M. S. (2005). Role of organic coating on carbonyl iron suspended particles in magnetorheological fluids. *J. Appl. Phys.* 97:10Q912. doi: 10.1063/1.1853835
- Kang, T. G., Hulsen, M. A., and den Toonder, J. M. (2012). Dynamics of magnetic chains in a shear flow under the influence of a uniform magnetic field. *Phys. Fluids* 24:042001. doi: 10.1063/1.4704822
- Kim, M. S., Liu, Y. D., Park, B. J., You, C.-Y., and Choi, H. J. (2012). Carbonyl iron particles dispersed in a polymer solution and their rheological characteristics under applied magnetic field. *J. Indus. Eng. Chem.* 18, 664–667. doi: 10.1016/j.jiec.2011.11.062
- Klingenberg, D. J., and Zukoski, C. F. (1990). Studies on the steady-shear behavior of electrorheological suspensions. *Langmuir* 6, 15–24. doi: 10.1021/la00091a003
- Kordonski, W. I., and Golini, D. (1999). Fundamentals of Magnetorheological fluid utilization in high precision finishing. *J. Intell. Mater. Syst. Struct.* 10, 683–689. doi: 10.1106/011M-CJ25-64QC-F3A6
- Laciš, S., and Gosko, D. (2009). Direct numerical simulation of MR suspension: the role of viscous and magnetic interactions between particles. *J. Phys.* 149:012066. doi: 10.1088/1742-6596/149/1/012066
- Laun, H. M., Gabriel, C., and Kieburg, C. (2010). Twin gap magnetorheometer using ferromagnetic steel plates—performance and validation. *J. Rheol.* 54, 327–354. doi: 10.1122/1.3302804
- Lim, S. T., Cho, M. S., Jang, I. B., and Choi, H. J. (2004). Magnetorheological characterization of carbonyl iron based suspension stabilized by fumed silica. *J. Magnetism Magnetic Mater.* 282, 170–173. doi: 10.1016/j.jmmm.2004.04.040
- Lootens, D., Van Damme, H., and Hébraud, P. (2003). Giant stress fluctuations at the jamming transition. *Phys. Rev. Lett.* 90:178301. doi: 10.1103/PhysRevLett.90.178301
- López-López, M. T., Kuzhir, P., Caballero-Hernandez, J., Rodríguez-Arco, L., Durán, J. D., and Bossis, G. (2012). Yield stress in magnetorheological suspensions near the limit of maximum-packing fraction. *J. Rheol.* 56:1209. doi: 10.1122/1.4731659
- Mari, R., Seto, R., Morris, J. F., and Denn, M. M. (2014). Shear thickening, frictionless and frictional rheologies in non-Brownian suspensions. *J. Rheol.* 58, 1693–1724. doi: 10.1122/1.4890747
- Pan, Z., de Cagny, H., Weber, B., and Bonn, D. (2015). S-shaped flow curves of shear thickening suspensions: Direct observation of frictional rheology. *Phys. Rev. E* 92:032202. doi: 10.1103/PhysRevE.92.032202
- Plachy, T., Kutalkova, E., Sedlacik, M., Vesel, A., Masar, M., and Kuritka, I. (2018). Impact of corrosion process of carbonyl iron particles on magnetorheological behavior of their suspensions. *J. Indus. Eng. Chem.* 66, 362–369. doi: 10.1016/j.jiec.2018.06.002
- Scales, P. J., Johnson, S. B., Healy, T. W., and Kapur, P. C. (1998). Shear yield stress of partially flocculated colloidal suspensions. *AIChE J.* 44, 538–544. doi: 10.1002/aic.690440305
- Suzuki, M., Makino, K., Yamada, M., and Linoya, K. (1981). A study on the coordination number in a system of randomly packed uniform sized spheres. *Int. Chem. Eng.* 21, 482–488.
- Tao, R. (2001). Super-strong magnetorheological fluids. *J. Phys.* 13, R979–R99. doi: 10.1088/0953-8984/13/50/202
- Wyart, M., and Cates, M. E. (2014). Discontinuous shear thickening without inertia in dense non-Brownian suspensions. *Phys. Rev. Lett.* 112:098302. doi: 10.1103/PhysRevLett.112.098302

Conflict of Interest Statement: The authors declare that the research was conducted in the absence of any commercial or financial relationships that could be construed as a potential conflict of interest.

Copyright © 2019 Bossis, Volkova, Grasselli and Cifre. This is an open-access article distributed under the terms of the Creative Commons Attribution License (CC BY). The use, distribution or reproduction in other forums is permitted, provided the original author(s) and the copyright owner(s) are credited and that the original publication in this journal is cited, in accordance with accepted academic practice. No use, distribution or reproduction is permitted which does not comply with these terms.